Published in final edited form as:
Environ Sci Technol. 2008 September 15; 42(18): 6936–6941.

Ligand-Enhanced Reactive Oxidant Generation by Nanoparticulate Zero-Valent Iron and Oxygen

Christina R. Keenan and **David L. Sedlak***
Department of Civil and Environmental Engineering, University of California at Berkeley, Berkeley, California 94720

Abstract

The reaction of zero-valent iron or ferrous iron with oxygen produces reactive oxidants capable of oxidizing organic compounds. However, the oxidant yield in the absence of ligands is too low for practical applications. The addition of oxalate, nitrilotriacetic acid (NTA), or ethylenediaminetetraacetic acid (EDTA) to oxygen-containing solutions of nanoparticulate zero-valent iron (nZVI) significantly increases oxidant yield, with yields approaching their theoretical maxima near neutral pH. These ligands improve oxidant production by limiting iron precipitation and by accelerating the rates of key reactions, including ferrous iron oxidation by oxygen and hydrogen peroxide. Product yields indicate that the oxic nZVI system produces hydroxyl radical (OH·) over the entire pH range in the presence of oxalate and NTA. In the presence of EDTA, probe compound oxidation is attributed to OH· under acidic conditions and a mixture of OH· and ferryl ion (Fe[IV]) at circumneutral pH.

Introduction

The reaction of granular or nanoparticulate zero-valent iron (ZVI or $Fe^0_{(s)}$) and oxygen (O_2) can produce reactive oxidants capable of oxidizing arsenic(III), pesticides, aromatic compounds, and chelating agents (1-6). In the absence of ligands, oxidation at acidic pH values is attributable to the generation of hydrogen peroxide (H_2O_2) during ZVI oxidation, which then reacts with ferrous iron (Fe[II]) via the Fenton reaction to produce hydroxyl radical (OH·; 7). At neutral pH values, Fe(II) oxidation by O_2 produces a different oxidant, most likely the ferryl ion (Fe[IV]; 7-8). The oxidant produced at neutral pH values can oxidize methanol and ethanol, but is unable to oxidize aromatic compounds.

In the absence of ligands, yields of species capable of oxidizing organic compounds in the ZVI/O_2 system are too low to be useful for remediation applications (e.g., approximately 7% of the ZVI is converted to Fe(IV) at pH 7 under optimal conditions; 7). Furthermore, OH· production requires acidification, which is often impractical in treatment systems. Several investigators have reported substantially increased reaction rates when ligands were added to either ZVI/O_2 or Fenton's reagent systems (e.g., 4,9). For example, chlorophenol oxidation by granular ZVI/O_2 was greatly enhanced by EDTA addition (4). When EDTA was present at high concentrations or when chlorophenol was absent, the ligand was transformed as ZVI was oxidized by O_2 (5-6). While the ZVI studies (4-6) provide evidence that ligands enhance reaction rates and yields, they provide little insight into the reaction mechanism or the effect of ligand concentration or pH on reaction rates and oxidant yields.

*Corresponding author e-mail: sedlak@ce.berkeley.edu; telephone: (510) 643-0256; fax: (510) 642-7483.

In this study, the oxidation of several organic compounds was studied under well-controlled conditions to provide insight into the ability of oxalate, NTA, and EDTA to enhance oxidant yields in the nanoparticulate ZVI/O_2 system under conditions that may be applied in an oxidative treatment process. Benzoic acid and 2-propanol were used to quantify the production of OH·, while methanol was used to quantify weaker oxidants, such as Fe(IV), as described previously (7).

Materials and Methods

Materials

All chemicals were reagent grade and were used as received except for 2,4-dinitrophenyl hydrazine (DNPH), which was recrystallized three times from acetonitrile. All solutions were prepared using 18 MΩ Milli-Q water from a Millipore system. Glassware was acid-washed and rinsed before use.

The following buffers were used: sodium acetate (pH 4-5), 2-(N-morpholino)ethanesulfonic acid (MES; pH 6), piperazine-N,N'-bis(ethanesulfonic acid) (PIPES; pH 7), and sodium borate (pH 8-9). All buffer concentrations were 1 mM. Solutions at pH 3 were unbuffered. MES and PIPES were selected because they do not form complexes with Fe(II) or Fe(III) under these conditions (10). The ligands were added as sodium oxalate, nitrilotriacetic acid (NTA), and ethylenediaminetetracetic acid (EDTA).

Nanoparticulate zero-valent iron (nZVI) was prepared daily as described previously to produce primary particles with a diameter between 10 and 100 nm and a surface area of 33.5 m^2/g (11). Ferrous iron stock solutions were prepared by dissolving ferrous sulfate in N_2-sparged 1 mM HNO_3.

Experimental Setup

All experiments were carried out at room temperature (20 ± 2°C) in the dark in 60-mL glass serum vials. The vials were sealed with rubber septa and had no headspace. Although the concentration of oxygen decreased as iron was oxidized, the final O_2 concentration was never less than 80 μM. To initiate a reaction, an aliquot of nZVI and/or Fe(II) (150 μM ± 15 μM) was added from a stock solution to air-saturated solutions containing the probe compound, ligand, and a buffer. The particles were kept in suspension by placing the reactors on an orbital shaker table at 150 rotations per minute. Samples were collected using a 5-mL glass syringe and filtered immediately through a 0.22-μm nylon syringe filter. The reactors were sacrificial, at least three reactors were sampled for each data point, and the data were averaged.

Analytical Techniques

A modified ferrozine method (7,12), was used to determine the concentration of filterable Fe (II), total filterable iron, and total iron in experiments without EDTA. The Fe^{III}EDTA complex was measured directly by UV absorption (13) or by HPLC (14-15). Details are included in Supporting Information. For both Fe^{III}EDTA methods, the standard curves were linear with regression coefficients >0.9990 and detection limits of 5 μM.

The main products from the oxidation of probe compounds were measured by HPLC as described previously (7). High concentrations of methanol and 2-propanol (100 mM) were used to ensure that >98% of the oxidants reacted with the probe compound to produce formaldehyde (HCHO) and acetone, respectively. A lower concentration of benzoic acid (5 mM) was used due to its limited solubility, ensuring that >80-95% of the oxidants reacted with the probe compound depending on the buffer and ligand selected. Benzoic acid reacts with OH· to form three isomers of hydroxybenzoic acid (ortho, meta, and para) that occur in the

ratio 36:34:30 based on a study using H_2O_2 photolysis as an OH· source (16), and total hydroxybenzoic acid yield was estimated from this ratio using measurements of para-hydroxybenzoic acid (pHBA). Product yield percentages in the text refer to the measured product concentration relative to the concentration of oxidized iron (i.e., $[Fe^0_{(s)}]_{initial}$ - [Fe (II)]$_{t=60}$).

Results

The addition of oxalate, NTA, and EDTA to the nZVI and oxygen system increased the yield of formaldehyde from methanol oxidation (Figure 1). HCHO production increased with increasing oxalate and NTA concentrations; higher concentrations of oxalate were needed due to weaker complexation with Fe(II). The maximum HCHO yield in the presence of EDTA was observed near the 1:1 ratio of EDTA:nZVI, with yields decreasing by approximately 35% as the EDTA concentration increased past this ratio. All subsequent experiments were conducted at concentrations where the maximum HCHO yields were observed (i.e., [oxalate] = 10 mM; [NTA] = 1 mM; [EDTA] = 0.2 mM).

Oxidant yield by nZVI and Fe(II) in the presence of 10 mM oxalate was determined using methanol, 2-propanol, and benzoic acid as probe compounds (Figure 2). Product yields were significantly higher relative to previous studies conducted in the absence of ligands (i.e., product yields were always less than 10 μM under similar conditions in the ligand-free nZVI/O_2 system; 7). Formaldehyde and acetone production was highest at pH 6, with yields of 26.0% and 29.4% relative to Fe oxidized, respectively (Figure 2a). The lower yield of HCHO following OH· exposure under acidic conditions is consistent with previous experiments (7). The maximum HBA yield (22.9%) was observed at pH 5, although the trend of maximum yields near neutral pH and decreased yields at extreme pH values was similar to that observed for the other two probe compounds (Figure 2a). The production of HCHO, acetone, and HBA when Fe(II) was exposed to O_2 was nearly identical to product generation by nZVI over the entire pH range (Figure 2b).

As was the case for oxalate, the presence of NTA (1 mM) and nZVI or Fe(II) (150 μM) resulted in higher yields of oxidized products over the entire pH range studied relative to previous studies conducted in the absence of ligands (Figure 3; 7). In the nZVI system, the maximum HCHO yield of 40.6% was observed at pH 8, while the maximum acetone and HBA yields of 40.1% and 22.8% were observed at pH 7 (Figure 3a). Although the oxidation of Fe(II) by O_2 produced product yields that followed the same qualitative trends as the oxidation of nZVI, the concentration of products formed was significantly lower for all three probe compounds (Figure 3b). For example, HCHO, acetone, and HBA production by Fe(II) was approximately 34.6%, 51.5%, and 71.3% of the yields generated by the same concentration of nZVI at pH 7.

EDTA addition also increased oxidized product yields over the entire pH range (Figure 4), but the product patterns were quite different among the three probe compounds. HCHO generation in the nZVI system followed a similar trend to that observed with the addition of oxalate and NTA; highest yields were observed near neutral pH (26.4% at pH 8), with lower yields observed under acidic and basic conditions (Figure 4a). However, the production of acetone and HBA was highest at pH 3 (32.7% and 12.0%) and decreased as pH increased (Figure 4a). There was still significant acetone and HBA generation at higher pH values (19.8% and 4.1% at pH 8). HCHO production by Fe(II) was similar to production by nZVI. Acetone and HBA yields from the reaction of Fe(II) with O_2 were very different than yields by nZVI, with maximum yields near neutral pH (Figure 4b). EDTA degradation was negligible in the presence of methanol, but increased with pH in the presence of 2-propanol and benzoic acid (Figure S1).

Ligand addition enhanced Fe(II) oxidation by O_2 (Figure 5a) over the entire pH range studied. In the absence of ligands, Fe(II) oxidation during a period of 60 min is negligible at pH 3 (7, 17). In the presence of 10 mM oxalate and 1 mM NTA at pH 3, Fe(II) was oxidized with half-lives of ~110 min and ~55 min under these experimental conditions (Figures S3, S4). Fe(II) was still detected after 180 minutes in both cases (26.9% in oxalate; 4.0% in NTA), and HCHO production occurred throughout the entire period (Figures S3, S4). The Fe(II) concentration measured after 60 min in the presence of oxalate or NTA was lower than the concentration observed in the absence of ligands at pH values from 3 to 6 (Figure 5a). Above pH 7, Fe(II) oxidation was complete within 60 minutes in all cases (Figures 5a, S3, S4).

The presence of oxalate, NTA, and EDTA increased the filterable iron concentration relative to the ligand-free case (Figure 5b). Iron solubility decreased with increasing pH in the absence of ligands, with very little iron remaining in solution by pH 7. The addition of 10 mM oxalate increased iron solubility in neutral conditions, with 29.7% of iron added remaining in solution after 60 min at pH 7. EDTA further increased iron solubility, with 53% remaining in solution after 60 min at pH 8. Iron was nearly completely filterable between pH 3-8 when 1 mM NTA was added. In the case of all three ligands, less filterable iron was present after 60 min in experiments in which iron was added as nZVI compared to experiments in which ferrous iron was added directly (Figure S2).

Discussion

In the nZVI/O_2 system, $Fe^0_{(s)}$ is oxidized to produce ferrous iron and H_2O_2 or H_2O (via reaction 1 or 2). H_2O_2 may also be produced by the reaction of ferrous iron and oxygen, followed by reaction of superoxide ($O_2^{\cdot -}$) with Fe(II) (reactions 3-4; 7):

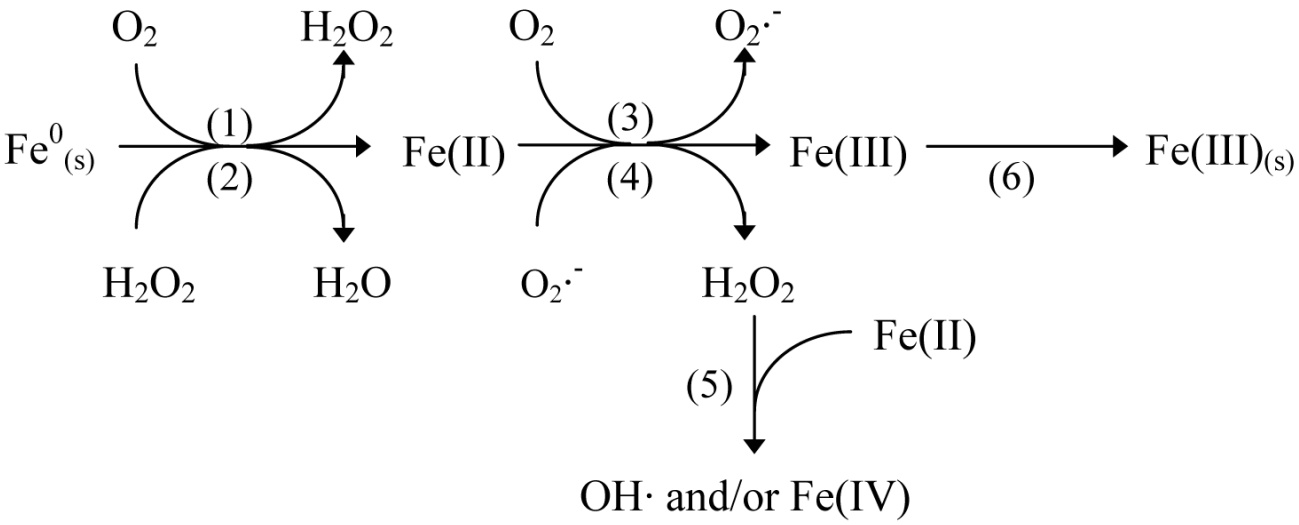

In this simplified scheme, Fe(II) and Fe(III) represent the sum of all free and hydrolyzed or complexed ferrous and ferric species. In the absence of ligands, reaction 1 is responsible for H_2O_2 production under acidic conditions and reactions 3-4 become the dominant H_2O_2 source at pH values above 5 (7). H_2O_2 reacts with either $Fe_{(s)}^0$ or Fe(II) (reactions 2, 5). If H_2O_2 reacts with $Fe^0_{(s)}$ (reaction 2), probe compound oxidation does not occur and the net reaction is:

$$2Fe^0_{(s)} + O_2 + 4H^+ \rightarrow 2Fe(II) + 2H_2O \quad (7)$$

If H_2O_2 reacts with Fe(II) (the Fenton reaction; reaction 5), an oxidant (i.e., hydroxyl radical or the ferryl ion) will be produced. The oxidant produced by reaction 5 depends upon Fe(II) speciation and can be quantified by measuring the oxidation products of different probe compounds. Following reaction 3, 4, or 5, Fe(III) may precipitate to form a ferric oxide or hydroxide (reaction 6). Precipitation of $Fe(III)_{(s)}$ could affect the other reactions by forming oxide layers on $Fe^0_{(s)}$ or acting as a surface catalyst for the oxidation of Fe(II) by O_2 or H_2O_2. The nZVI/O_2 system is defined by reactions 1-6, while only reactions 3-6 are possible in the Fe(II)/O_2 system. Dissolution of nZVI (reactions 1-2) may influence the kinetics of subsequent reactions.

The addition of ligands may alter oxidant production in several ways. First, complexation may accelerate the Fenton reaction (reaction 5), increasing the branching ratio between reactions 2 and 5 and allowing a larger fraction of H_2O_2 to produce oxidants. Second, precipitation of $Fe(III)_{(s)}$ (reaction 6) may lead to co-precipitation of Fe(II) or passivation of the nZVI surface, which could decrease product yields. Complexation of Fe(III) by ligands can enhance Fe(III) solubility. Third, ferrous iron oxidation by oxygen is strongly pH dependent and is negligible at pH values below 5 in the absence of ligands over the one hour duration of these experiments (reaction 3; 7, 17). Accelerating reaction 3 by complexation may increase the yield of H_2O_2. Finally, coordination of the metal may alter the nature of the reactive oxidant produced in reaction 5 (18). Detailed discussion on how each ligand alters the reaction mechanism and improves oxidant yield is presented in order of increasing system complexity.

Oxalate

Oxalate ($C_2O_4^{2-}$) forms a bidentate complex with ferrous iron. In 10 mM oxalate, $FeC_2O_4^0$ accounts for 34.9% (pH 3), 67.2% (pH 4), and >77% (pH 5-9) of Fe(II) (Figure S6). Despite the relatively high concentration of oxalate needed to enhance oxidant production, the low reactivity of $C_2O_4^{2-}$ with OH· ($k = 7.7 \times 10^6\ M^{-1}s^{-1}$; 19) ensured that oxalate did not out compete the probe compounds for OH·.

The presence of oxalate in the nZVI system increased oxidant production by altering the reaction mechanism in several ways (Figure 2). First, the reaction of H_2O_2 and $Fe(C_2O_4)^0$ is three orders of magnitude faster than the reaction of H_2O_2 and Fe^{2+} (reaction 5; 20). Therefore, a larger fraction of the H_2O_2 produced by reactions 1 and 4 was converted to oxidants (i.e., the rate of reaction 5 increased relative to reaction 2). Second, the presence of oxalate increases the solubility of Fe(III) through formation of Fe(III)-oxalate complexes at pH <8 (Figure 5b). The measured concentration of filterable iron in the presence of oxalate agreed well with equilibrium calculations (Figure S6), which predicted oversaturation with respect to ferrihydrite above pH 7.

Third, oxalate complexation increases the rate of ferrous iron oxidation by O_2 (reaction 3), notably under acidic conditions. In the presence of 10 mM oxalate, ferrous iron was oxidized with a half-life of ~110 minutes at pH 3 (Figures S3, S4). The generation of HCHO, acetone, and HBA by nZVI and Fe(II) were nearly identical (Figure 2). Thus, reactions 3-4 are the main source of H_2O_2 production over the entire pH range and nZVI simply served as a source of Fe (II). The maximum possible yield of oxidants from Fe(II) oxidation (reactions 3-5) is 33%, or one mole of oxidant produced per three moles of iron consumed (i.e., 50 μM). Product yields were near this value for acetone and HBA at pH values below 7 (i.e., as long as Fe(III) did not precipitate). Formaldehyde yields approached the theoretical maximum at pH 6 and 7. At lower pH values, HCHO yields decreased relative to acetone and HBA yields due to inefficient conversion of methanol to HCHO by OH·(7).

Finally, the complexation of Fe(II) by oxalate alters the nature of the reactive oxidant produced via the Fenton reaction (reaction 4). Because HCHO, acetone and HBA production followed

the same trends and approached the theoretical maximum over the pH range studied (Figure 2), we conclude that OH· is the dominant oxidant species produced.

NTA

Nitrilotriacetic acid is an aminopolycarboxylate ligand that forms tetradentate complexes with iron. Equilibrium calculations predict nearly complete complexation of both dissolved ferrous and ferric iron at neutral pH in 1 mM NTA (Figure S7). The Fe(II)-NTA complex has at least one coordinated water molecule, enabling reactions with O_2 and H_2O_2 (21). The addition of NTA to the nZVI and O_2 system increases oxidant yield substantially through the same processes acting in the oxalate system (Figure 3). First, iron-NTA complexes show higher reactivity with H_2O_2 relative to free iron and iron-EDTA complexes over a broad range of pH (9, 21-22). The accelerated rate of the Fenton reaction (reaction 5) favors the formation of reactive oxidants.

Second, 150 μM of iron was almost completely filterable over the entire pH range studied in the presence of 1 mM NTA (Figure 5b). Equilibrium calculations predict oversaturation with respect to ferrihydrite above pH 7 in the presence of 1 mM NTA (Figure S7); however, the presence of excess NTA limited ferrihydrite precipitation during the experimental time scale. Filterable Fe decreased by 34% between 60 min and 260 min in the nZVI/O_2/NTA system (data not shown), suggesting that the system was oversaturated but that filterable colloids were still forming at 60 min.

Third, the rate of ferrous iron oxidation by O_2 (reaction 3) is significantly increased in the presence of NTA (13, 23). Ferrous iron was oxidized with a half-life of 55 minutes in 1 mM NTA at pH 3 (Figure S4). In the Fe(II)/O_2/NTA system the yields of HCHO, acetone, and HBA were about 60% of the theoretical maximum (i.e., 33% or 50 μM) at pH values between 6 and 8. At lower pH values, yields decreased due to incomplete Fe(II) oxidation and limited conversion of methanol to HCHO by OH·. The maximum yields in the nZVI/O_2/NTA system were approximately twice as high as those observed in the Fe(II)/O_2/NTA system, suggesting that NTA increased the yield of H_2O_2 from reaction 1. The maximum possible yield of oxidants is 100% (i.e., reaction 1 followed by reaction 5). The highest product yields observed here were ~40% (Figure 3), further supporting a combination of reactions 1 and 3-4, followed by reaction 5.

As was the case with oxalate, NTA alters the reactive oxidant, resulting in production of OH· over the entire pH range as seen from the agreement in HCHO, acetone, and HBA yields (Figure 3). HBA generation was slightly lower than acetone generation at pH 6 and 7, most likely due to scavenging of OH· by the organic buffers MES and PIPES (up to 17% of OH· reacted with the buffer; Table S1).

EDTA

The iron EDTA system is complicated by pH-dependent changes in speciation (Figure S8), slow complex formation kinetics (24-25), slow kinetics of Fe-EDTA complex dissolution from solid iron species (26-27), and the possibility of EDTA degradation in the ZVI/O_2 systems (5-6). Although the coordination geometry of $Fe^{II/III}$EDTA is uncertain, it is believed to include at least one labile water molecule, as evidenced by the reaction of Fe-EDTA complexes with O_2 (28-29) and H_2O_2 (21).

The addition of EDTA to nZVI-containing solutions increased production of HCHO, acetone, and HBA relative to the ligand-free system over the entire pH range studied (Figure 4; 7). HCHO production was highest when the EDTA concentration was approximately equal to the amount of nZVI added (Figure 1), and decreased as the EDTA:nZVI ratio increased above 1:1.

In Fenton systems, high ratios of EDTA:Fe(II) (e.g., > 2:1) can inhibit the reduction of H_2O_2 (30). A similar decrease in EDTA degradation rates by granular ZVI in the presence of excess EDTA was attributed to the prevention of the formation of the H_2O_2-$Fe^{II/III}$EDTA and O_2-$Fe^{II/III}$-EDTA adducts necessary for oxidant production (5).

An increase in oxidant yield due to the presence of EDTA may be attributable to the same factors that led to increases in yields by oxalate and NTA. First, studies on the addition of H_2O_2 to solutions containing Fe(II) and EDTA suggest that the Fenton reaction is accelerated over a broad range of pH when iron is complexed with EDTA (22,24,31). Second, the presence of EDTA resulted in increased iron solubility at all pH values (Figure 5b). Equilibrium calculations indicated that 150 μM Fe(III) would be soluble at all pH values in the presence of 200 μM EDTA (Figure S8). While this was true at pH values <9 when Fe was added as Fe(II) (Figure S2), only 48.7% Fe was filterable at pH 7 after 60 min when Fe was added as nZVI (Figure 5b). Filterable Fe increased with time (63.0% filterable after 180 min at pH 7; Figure S5) in agreement with observations that dissociation of Fe-EDTA complexes from solids such as hydrous ferric oxide (26) and granular ZVI (27) are kinetically limited.

The rate of oxidation of Fe(II) by oxygen is significantly enhanced in the presence of EDTA (Reaction 3; 28-29, 32). Oxidation is fastest near pH 3 ($t_{1/2} \sim 0.1$ sec) and independent of pH at pH values above 5 ($t_{1/2} \sim 1$ sec; 28-29), suggesting that oxidation of Fe(II) in the presence of EDTA was almost instantaneous under the experimental conditions employed in this study.

The relative contribution of reactions 1 and 3-4 to H_2O_2 production by nZVI and EDTA is unclear. Unlike observations for oxalate and NTA, the production of HCHO, acetone and HBA by nZVI and Fe(II) in the presence of EDTA did not always agree (Figure 4). Acetone and HBA generation by Fe(II) and EDTA were highest near neutral pH, following the same trend as HCHO production. HCHO production at pH 9 was higher when iron was added as Fe(II) instead of as nZVI due to increased iron solubility in the Fe(II) system (Figures 4, 5b, and S2). Although these results are inconclusive, it is clear that production of reactive oxidants by nZVI and EDTA is not simply due to Fe(II) oxidation (reactions 3-4) and that the presence of surfaces plays a role in enhanced oxidant production.

The trends in HCHO, acetone, and HBA production and EDTA degradation in the nZVI/O_2/EDTA system provide insight into the nature of the reactive oxidant(s) produced. All three products were present under acidic conditions, suggesting that OH· was the main oxidant generated (Figure 4). Acetone and HBA production decreased as pH increased, while HCHO production increased at neutral pH values. In addition, EDTA degradation was minimal in the presence of methanol and increased with increasing pH in the presence of 2-propanol and benzoic acid (up to 9% EDTA degradation at pH 9; Figure S1). This suggests that a reactive oxidant capable of reacting with methanol and EDTA, such as the ferryl ion, may be present. However, significant amounts of acetone and HBA were present after 60 min at pH 7 (Figure 4), suggesting that a mixture of Fe(IV) and OH· is produced. HCHO, acetone, and HBA yields by Fe(II) in the presence of EDTA were highest near neutral pH (Figure 4), suggesting that OH· is produced in the absence of nZVI surfaces.

There are conflicting reports on the type of oxidant produced by Fe^{II}EDTA and O_2 or H_2O_2. Some researchers have found evidence supporting the presence of an alternate oxidant such as Fe(IV) (ZVI/O_2/EDTA, *6;* Fe(II)/O_2/EDTA, *23*; Fe(II)/H_2O_2/EDTA, 33), while others have found evidence of OH· (ZVI/O_2/EDTA, 5) or a mixture of OH· and Fe(IV) (Fe(II)/O_2/H_2O_2/EDTA, 34). The type of oxidant produced by iron chelated by EDTA appears to be sensitive to numerous solution conditions, including pH, the ratio of EDTA:Fe, the presence of surfaces, and the concentration of O_2 or H_2O_2. For example, Sun and Pignatello (Fe(III)/H_2O_2/EDTA, 9) described EDTA as inactive in their study on 2,4-D degradation in the Fenton system at pH

6, contrary to other work suggesting that iron-EDTA complexes are amenable to reaction with H_2O_2. It may be that the system produced Fe(IV) at this pH and that the oxidant was unable to react with the aromatic contaminant. Conversely, Noradoun *et al.* (ZVI/O_2/EDTA, 4) observed oxidation of recalcitrant chlorophenols in the presence of granular ZVI and EDTA in an unbuffered system where the pH ranged from 5.5-6.5. In those experiments, chlorophenol degradation may have been due to OH· production at the lower pH values.

Implications for Contaminant Oxidation

Ligands provide a possible means of using nZVI or Fe(II) and oxygen for oxidative treatment of contaminants. The addition of oxalate, NTA, and EDTA significantly increased reactive oxidant yields over a broad pH range by accelerating the rates of key reactions (e.g., Fe(II) oxidation by O_2 and H_2O_2) and increasing ferric iron solubility. Oxalate and NTA favor the formation of OH· rather than Fe(IV) at neutral pH, potentially enabling the oxidation of a wide range of contaminants at neutral pH values. However, relatively high concentrations of oxalate were required and it may not be practical to discharge high concentrations of NTA to the aquatic environment. Although only a small concentration of EDTA was needed to improve oxidant yield, the formation of an oxidant other than OH· (e.g., Fe[IV]), the possibility of EDTA degradation, and the ability of EDTA to mobilize toxic metals suggest that it may not be an ideal additive to the nZVI/O_2 system unless EDTA is the target contaminant (e.g., 5-6).

Supplementary Material

Refer to Web version on PubMed Central for supplementary material.

Acknowledgements

This research was supported by the U.S. National Institute for Environmental Health Services (Grant E5004705). We thank Changha Lee for his advice.

Literature Cited

(1). Leupin OX, Hug SJ. Oxidation and removal of arsenic(III) from aerated groundwater by filtration through sand and zero-valent iron. Water Res 2005;39:1729–1740. [PubMed: 15899271]

(2). Joo SH, Feitz AJ, Waite TD. Oxidative degradation of the carbothioate herbicide, molinate, using nanoscale zero-valent iron. Environ. Sci. Technol 2004;38:2242–2247. [PubMed: 15112830]

(3). Joo SH, Feitz AJ, Sedlak DL, Waite TD. Quantification of the oxidizing capacity of nanoparticulate zero-valent iron. Environ Sci. Technol 2005;39:1263–1268. [PubMed: 15787365]

(4). Noradoun C, Engelmann MD, McLaughlin M, Hutcheson R, Breen K, Paszczynski A, Cheng IF. Destruction of chlorinated phenols by dioxygen activation under aqueous room temperature and pressure conditions. Ind. Eng. Chem. Res 2003;42:5024–5030.

(5). Noradoun CE, Cheng IF. EDTA degradation induced by oxygen activation in a zerovalent iron/air/water system. Environ. Sci. Technol 2005;39:7158–7163. [PubMed: 16201643]

(6). Englehardt JD, Meeroff DE, Echegoyen L, Deng Y, Raymo FM, Shibata T. Oxidation of aqueous EDTA and associated organics and coprecipitation of inorganics by ambient iron-mediated aeration. Environ. Sci. Technol 2007;41:270–276. [PubMed: 17265958]

(7). Keenan CR, Sedlak DL. Factors affecting the yield of oxidants from the reaction of nanoparticulate zero-valent iron and oxygen. Environ. Sci. Technol 2008;42:1262–1267. [PubMed: 18351103]

(8). Hug SJ, Leupin O. Iron-catalyzed oxidation of arsenic(III) by oxygen and by hydrogen peroxide: pH-dependent formation of oxidants in the Fenton reaction. Environ. Sci. Technol 2003;37:2734–2742. [PubMed: 12854713]

(9). Sun Y, Pignatello JJ. Chemical treatment of pesticide wastes. Evaluation of Fe(III) chelates for catalytic hydrogen peroxide oxidation of 2,4-D at circumneutral pH. J. Agric. Food Chem 1992;40:322–327.

(10). Yu Q, Kandegedara A, Xu YP, Rorabacher DB. Avoiding interferences from Good's buffers: A contiguous series of noncomplexing tertiary amine buffers covering the entire range of pH 3-11. Anal. Biochem 1997;253:50–56. [PubMed: 9356141]

(11). Nurmi JT, Tratnyek PG, Sarathy V, Baer DR, Amonette JE, Pecher K, Wang C, Linehan JC, Matson DW, Penn RL, Driessen MD. Characterization and properties of metallic iron nanoparticles: Spectroscopy, electrochemistry, and kinetics. Environ. Sci. Tecnhol 2005;39:1221–1230.

(12). Voelker BM, Sulzberger B. Effects of fulvic acid on Fe(II) oxidation by hydrogen peroxide. Environ. Sci. Technol 1996;30:1106–1114.

(13). Kurimura Y, Ochiai R, Matsuura N. Oxygen oxidation of ferrous ions induced by chelation. Bull. Chem. Soc. Jap 1968;41:2234–2239.

(14). Nowack B, Kari FG, Hilger SU, Sigg L. Determination of dissolved and adsorbed EDTA species in water and sediments by HPLC. Anal. Chem 1996;68:561–566.

(15). Ridge AC, Sedlak DL. Effect of ferric chloride addition on the removal of Cu and Zn complexes with EDTA during municipal wastewater treatment. Water Res 2004;38:921–932. [PubMed: 14769412]

(16). Zhou XL, Mopper K. Determination of photochemically produced hydroxyl radicals in seawater and freshwater. Mar. Chem 1990;30:71–88.

(17). Singer PL, Stumm W. Acidic mine drainage: The rate-determining step. Science 1970;167:1121–1123. [PubMed: 17829406]

(18). Goldstein S, Meyerstein D, Czapski G. The Fenton reagents. Free Rad. Biol. Med 1993;15:435–445. [PubMed: 8225025]

(19). Buxton GV, Greenstock CL, Helman WP; Ross AB. Critical review of rate constants for reactions of hydrated electrons, hydrogen atoms and hydroxyl radicals in aqueous solutions. J. Phys. Chem. Ref. Data 1988;17:513–886.

(20). Sedlak DL, Hoigné J. The role of copper and oxalate in the redox cycling of iron in atmospheric waters. Atmos. Environ 1993;27A:2173–2185.

(21). Graf E, Mahoney JR, Bryant RG, Eaton JW. Iron-catalyzed hydroxyl radical formation. J. Biol. Chem 1984;259:3620–3624. [PubMed: 6323433]

(22). Tachiev G, Roth JA, Bowers AR. Kinetics of hydrogen peroxide decomposition with complexed and "free" iron catalysts. Int. J. Chem. Kinet 2000;32:24–35.

(23). Welch KD, Davis TZ, Aust SD. Iron autoxidation and free radical generation: Effects of buffers, ligands, and chelators. Arch. Biochem. Biophys 2002;397:360–369. [PubMed: 11795895]

(24). Walling C, Kurz M, Schugar HJ. The iron(III)-ethylenediaminetetraacetic acid-peroxide system. Inorg. Chem 1970;9:931–937.

(25). Hudson RJM, Couvalt DT, Morel FMM. Investigations of iron coordination and redox reactions in seawater using Fe-59 radiometry and ion-pair solvent extraction of amphiphilic iron complexes. Mar. Chem 1992;38:209–235.

(26). Nowack B, Sigg L. Dissolution of Fe(III)(hydr)oxides by metal-EDTA complexes. Geochim. Cosmochim. Acta 1997;61:951–963.

(27). Pierce EM, Wellman DM, Lodge AM, Rodriguez EA. Experimental determination of the dissolution kinetics of zero-valent iron in the presence of organic complexants. Environ. Chem 2007;4:260–270.

(28). Zang V, van Eldik R. Kinetics and mechanism of the autoxidation of iron(II) induced through chelation by ethylenediaminetetraacetate and related ligands. Inorg. Chem 1990;29:1705–1711.

(29). Seibig S, van Eldik R. Kinetics of [Fe^{II}(edta)] oxidation by molecular oxygen revisited. New evidence for a multistep mechanism. Inorg. Chem 1997;36:4115–4120.

(30). Engelmann MD, Bobier RT, Hiatt T, Cheng IF. Variability of the Fenton reaction characteristics of the EDTA, DTPA, and citrate complexes of iron. Biometals 2003;16:519–527. [PubMed: 12779237]

(31). Wubs HJ, Beenackers ACM. Kinetics of the oxidation of ferrous chelates of EDTA and HEDTA in aqueous solution. Ind. Eng. Chem. Res 1993;32:2580–2594.

(32). Gambardella F, Ganzeveld IJ, Winkleman JGM, Heeres EJ. Kinetics of the reaction of Fe^{II}(EDTA) with oxygen in aqueous solutions. Ind. Eng. Chem. Res 2005;44:8190–8198.

(33). Rush JD, Koppenol WH. Oxidizing intermediates in the reaction of ferrous EDTA with hydrogen peroxide. J. Bio. Chem 1986;261:6730–6733. [PubMed: 3009473]

(34). Yamazaki I, Piette LH. EPR spin-trapping study on the oxidizing species formed in the reaction of the ferrous ion with hydrogen peroxide. J. Am. Chem. Soc 1991;113:7588–7593.

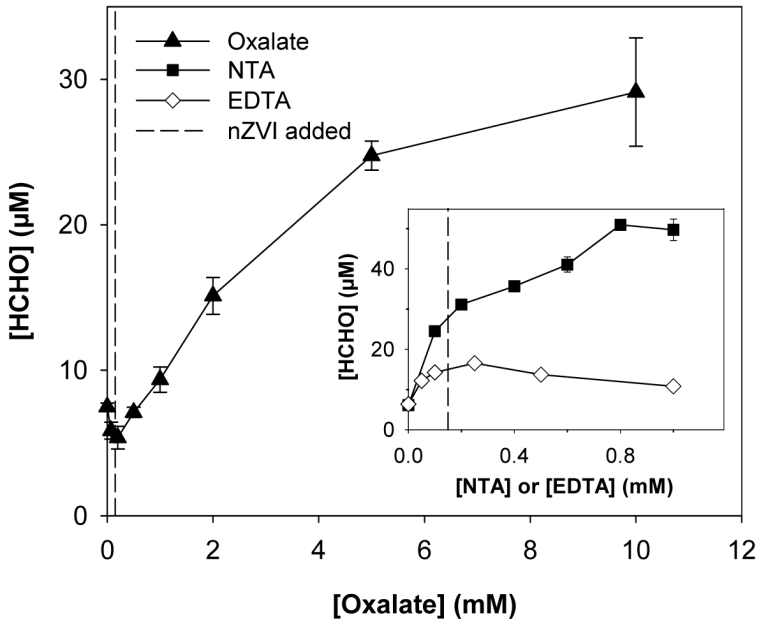

Figure 1.

HCHO yield after exposure of 150 μM nZVI to O_2 in the presence of oxalate, NTA (inset), or EDTA (inset) in 100 mM CH_3OH and 1 mM PIPES (pH 7, t = 60 min). The dashed line indicates the concentration of nZVI added.

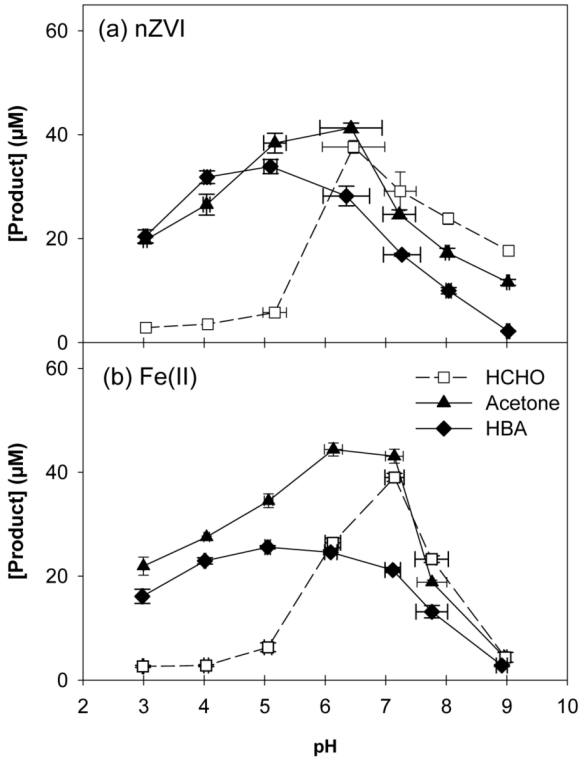

Figure 2.
Product yield after 60 min for (a) 150 μM nZVI + 10mM oxalate and (b) 150 μM Fe(II) + 10mM oxalate in 100 mM CH_3OH, 100 mM 2-propanol, and 10 mM benzoic acid.

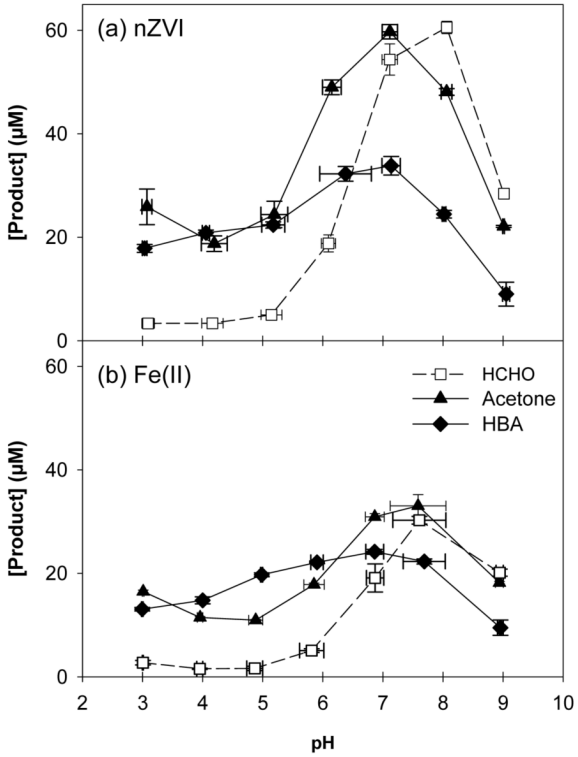

Figure 3.
Product yield after 60 min for (a) 150 μM nZVI + 1 mM NTA and (b) 150 μM Fe(II) + 1 mM NTA in 100 mM CH_3OH, 100 mM 2-propanol, and 10 mM benzoic acid.

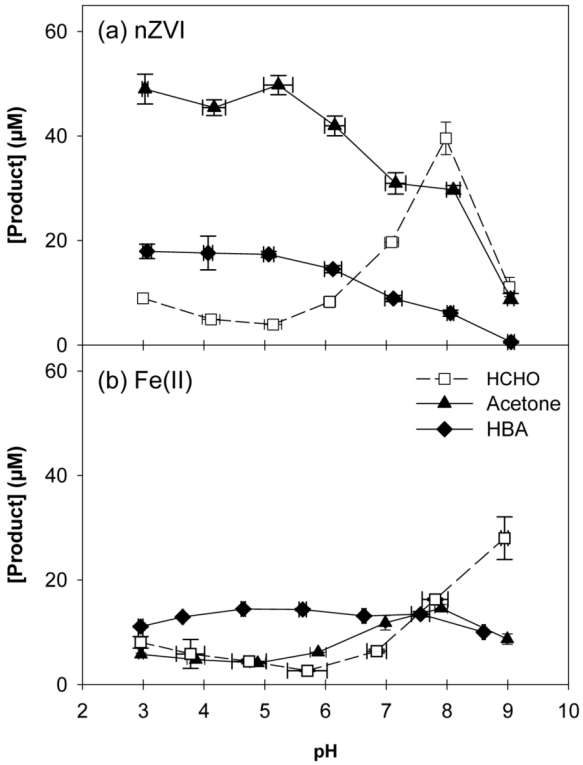

Figure 4.
Product yield after 60 min for (a) 150 μM nZVI + 200 μM EDTA and (b) 150 μM Fe(II) + 200 μM EDTA in 100 mM CH_3OH, 100 mM 2-propanol, and 10 mM benzoic acid.

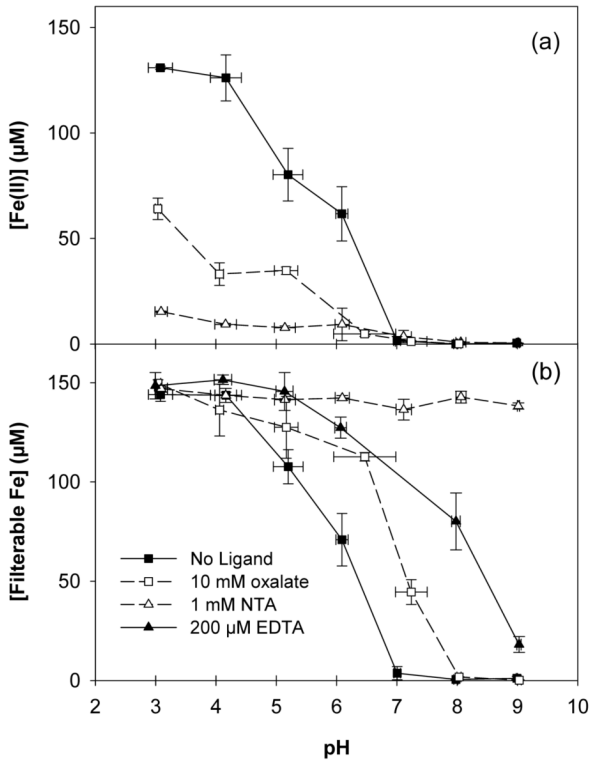

Figure 5.
(a) Fe(II) and (b) filterable Fe in 150 μM nZVI in 100 mM CH_3OH at 60 min. Data for no ligand, 10 mM oxalate, 1 mM NTA, and 200 μM EDTA. Initial pH as indicated.